Seismic scattering and attenuation properties of Mars estimated through coda analysis of S1222a marsquake, K. Onodera[1], T. Maeda[2], K. Nishida[1], T. Kawamura[3], S. Menina[3], L. Margerin[4], P. Lognonné[3], and W. B. Banerdt[5], [1]Earthquake Research Institute, The University of Tokyo (onodera@eri.u-tokyo.ac.jp), [2]Hirosaki University, [3]Institut de Physique du Globe de Paris, [4]Institut de Recherche en Astrophysique et Planétologie, Université Toulouse III Paul Sabatier, [5]Jet Propulsion Laboratory, California Institute of Technology

Introduction: In the past three years, NASA's InSight (Interior Exploration using Seismic Investigations, Geodesy, and Heat Transport) kept sending us high-quality seismic data from Mars and contributed to better understanding the seismicity and internal structure of the planet (e.g., [1]-[6]).

On the other hand, there remain lots of mysteries in the heterogeneous structures that hold valuable information to retrieve the past surface and/or internal evolution processes (e.g., volcanic activities, impact history). In seismology, it is known that the seismic scattering is associated with the internal heterogeneity and the quantitative evaluation of inhomogeneity has been performed by modeling the energy decay trend of scattered seismic waves (e.g. [7][8]).

In previous works [2][9][10], the Martian scattering and attenuation properties were assessed at the middle to high frequency (0.5 – 7.5 Hz), whereas those parameters are yet to be constrained at a low-frequency range (< 0.1 Hz). In this study, using the largest marsquake called S1222a [11], we give an initial estimation of scattering and attenuation factors at low frequency to fill the missing piece for a better illustration of the Martian heterogeneous structure.

The largest marsquake – S1222a: On May 4th-2022, the Very Broadband seismometer (VBB) installed by InSight [12] detected the largest marsquake during its operation. The notable features of S1222a are, in addition to clear body wave arrivals, strong excitations of surface waves such as Rayleigh and Love waves, which have been rarely confirmed in other marsquakes [11][13].

Figures 1a-c show the spectrogram, mean squared (MS) envelope, and filtered waveform of S1222a recorded by the vertical component of VBB. The red-filled area with R_1 is the arrival of Rayleigh wave propagating along the minor arc, which has been identified by Kawamura et al. [11]. The other red and green-filled areas (e.g., R_2, R_3 …) are the expected arrival times of multi-orbital phases.

In this study, we focus on the scattered Rayleigh waves at a frequency of 0.05 – 0.09 Hz, where the scattering and attenuation properties have not been constrained yet.

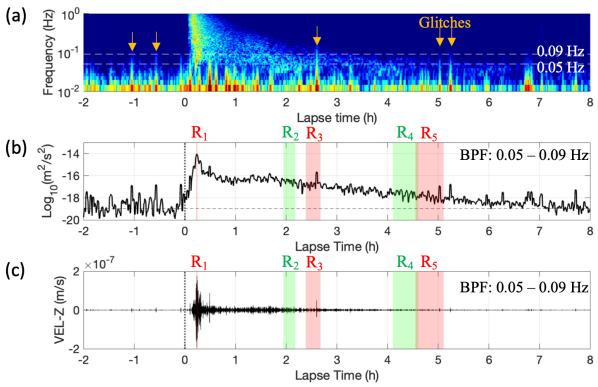

Figure 1. (a) Spectrogram of S1222a recorded with the vertical component of the very broad band seismometer. Orange arrows show the representative glitches in this period. The vertical axis shows the frequency covering from 0.01 to 1 Hz, and the horizontal shows the lapse time in hours from the origin time. (b) Mean squared (MS) envelope of S1222a filtered between 0.05 – 0.09 Hz. The red and green-filled areas are the expected arrival times of Rayleigh wave and its multi orbits. (c) Filtered waveform between 0.05 – 0.09 Hz.

Estimation of scattering and attenuation parameters: To retrieve the scattering and intrinsic quality factors (Q_i and Q_s) – the quantitative indicators of the seismic energy attenuation due to scattering and energy absorption by media, respectively, we employed the radiative transfer theory on a spherical body, which is a well-established approach in terrestrial seismology [14][15][16].

With the information about source and station locations reported by Kawamura et al. [11], we constructed the theoretical MS envelope model (see [14][15] for the details). The idea is to model the observed energy decay trend with the theoretical curve and then find preferable Q_i and Q_s to realize the best fit to the observation.

Figures 2a-b show how Q_i and Q_s affect the theoretical envelopes. Q_i mainly controls the energy decay rate and Q_s influences the energy peaks of the multi-orbital phases of Rayleigh wave.

By combining the radiative transfer modeling described above with some observational constraints such as no clear detection of multi-orbits in our target frequency range, we obtained the preferable Q_i and Q_s ranges as 1000 – 1500 and 30 – 500, respectively.

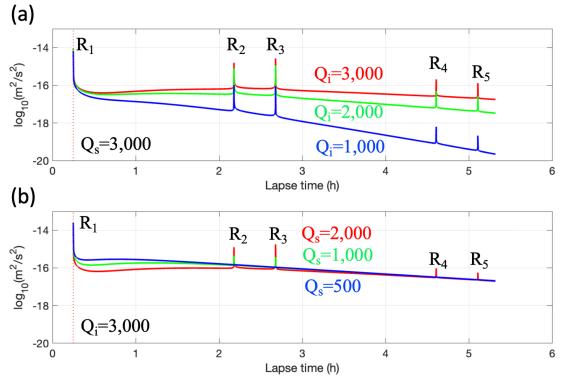

Figure 2. (a) Comparison of theoretical MS envelopes for the different Q_i with Q_s fixed to 3000. (b) Comparison of theoretical MS envelopes for the different Q_s with Q_i fixed to 3000.

Comparison between the Earth, the Moon, and Mars in terms of scattering intensity: Figure 3 displays the scattering quality factors obtained on three solid bodies (The comparison of the intrinsic Q will be presented in our future article). The smaller value indicates the stronger scattering. The summary of the terrestrial values can be found in [14][17][18]. The lunar values were referred from [19]-[22], and the previous estimations for Mars can be found in [2][9][23]. Our result is shown by orange-filled area at a frequency of 0.05 – 0.09 Hz.

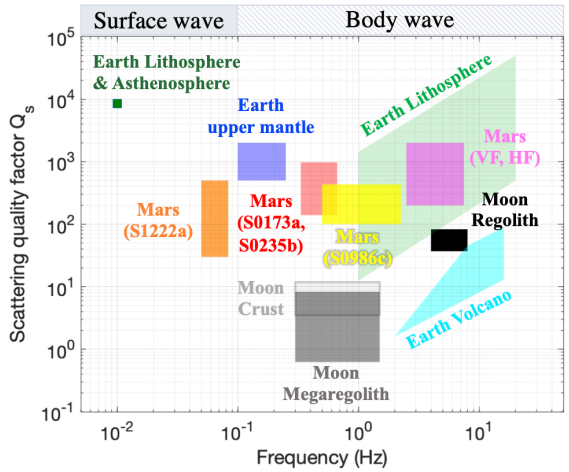

Figure 3. Comparison of scattering quality factor between the Earth, the Moon, and Mars. The plots below 0.1 Hz are for surface waves and those above 0.1 Hz are for body waves.

At high frequency (> 1 Hz), the Martian Q_s coincides with that of the Earth's lithosphere, indicating the scattering intensity is not as strong as those of the terrestrial volcanic regions or the near-surface of the Moon. In the middle frequency range (~0.5 Hz), the Martian value keeps the same intensity as that for the high-frequency range, which corresponds to tens time weaker scattering compared to the lunar crust and megaregolith. At lower frequency (< 0.1 Hz), our result for S1222a is compatible with other results for Mars, indicating that the Martian scattering intensity is similar to Earth's lithosphere.

Summary: In this study, we evaluated the scattering and attenuation properties of Mars by modeling the decay coda of S1222a with the radiative transfer theory on a spherical Mars. Consequently, we succeeded in retrieving the scattering properties, and also found that the Martian scattering intensity is comparable with that observed in the terrestrial lithosphere.

Acknowledgments: We acknowledge NASA, CNES, their partner agencies and Institutions (UKSA, SSO, DLR, JPL, IPGP-CNRS, ETHZ, IC, and MPS-MPG), and the flight operations team at JPL, SISMOC, MSDS, IRIS-DMC, and PDS for acquiring and providing InSight data, including SEED SEIS data.

References: **[1]** Banerdt et al. (2020), *Nat. Geosci.*, 13(3), 183-189. **[2]** Logononné et al. (2020), *Nat. Geosci.*, 13(3), 213-220. **[3]** Giardini et al. (2020), *Nat. Geosci.*, 13, 205-212. **[4]** Khan et al. (2021), *Science*, *373*(6553), 434-438. **[5]** Knapmeyer-Endrun et al. (2021), *Science*, 373(6553), 438-443. **[6]** Stähler et al. (2021), *Science*, *373*(6553), 443-448. **[7]** Aki (1969), *JGR* (1896 – 1977), 74 (2), 615-631. **[8]** Aki and Chouet (1975), *JGR (1896 – 1977)*, 80 (23), 3322-3342. **[9]** Menina et al. (2021), *BSSA*, *111*(6), 3016-3034. **[10]** Karakostas et al. (2021), *BSSA*, *111*(6), 3035-3054. **[11]** Kawamura et al. (2022), *GRL*, e2022GL101543. **[12]** Lognonné et al. (2019), *Space Sci. Rev.*, *215*(1), 12. **[13]** Kim et al. (2022), *Science*, 378(6618), 417-421. **[14]** Sato and Nohechi (2001), *JGR: Solid Earth*, *106*(B4), 6589-6594. **[15]** Sato and Nishino (2002), *JGR: Solid Earth*, *107*(B12) ESE 7-1 – ESE 7-9. **[16]** Maeda et al. (2006), *Pure and Applied Geophys.*, *163*(2), 549-566. **[17]** Sato et al. (2012), *Seismic wave propagation and scattering in the heterogeneous earth: 2nd edition*, Springer Berlin, Heidelberg. **[18]** Sato (2019), *GJI*, *218*(3), 2079-2088. **[19]** Blanchette-Guertin et al. (2012), *JGR: Planets*, 117 (E6). **[20]** Gillet et al. (2017), *PEPI, 262*, 28-40. **[21]** Onodera et al. (2022), *JGR: Planets*, e2022JE007558. **[22]** Nakamura (1976), *BSSA*, *66*(2), 593-606. **[23]** Garcia et al. (2022), *Nat. Geosci.*, *15*(10), 774-780.